



# Evaluation of the effect of waste zeolite on the strength and micro-macrostructure of a high plasticity clayey soil stabilized with lime-waste zeolite mixtures subjected to freezing–thawing cycles

Fatih Yılmaz<sup>1</sup> · Erol Sadoğlu<sup>2</sup> · Hakan Alper Kamiloğlu<sup>1</sup>

Received: 17 December 2021 / Accepted: 23 February 2022 / Published online: 8 March 2022  
© Saudi Society for Geosciences 2022

## Abstract

This study investigates the effect of waste zeolite (waste zeolite) and lime-waste zeolite mixtures on swelling potential, mechanical, and durability performances of a high plasticity clayey soil considering the macro and micro aspects. Three different subtypes of the tuffite formation were taken into account to examine the effect of differences of tuff structure on the stabilization performance. Within this scope, XRD, XRF, and SEM analyses were performed to identify mineralogical and oxide components of the materials. Computed tomography (CT) and scanning electron microscope (SEM) images were evaluated during the inner structure examination. The correlation between unconfined compressive strength and Hounsfield unit (HU) obtained from the CT images was investigated statistically. Pearson's correlation analysis and Spearman's Rho were performed to measure the strength of association between two variables. The swelling and mechanical properties of the stabilized soils were evaluated. Durability performances of the stabilized samples were determined considering unconfined compressive strength and the HU values of the samples subjected to freezing–thawing (F-T) cycles. The effects of curing and F-T cycles on the volume of the samples were investigated using CT imaging. The unconfined compressive strength of the natural soil at the end of the 28-day curing period was determined as 118.46 kPa, and the SLW10 sample containing natural soil + 6% lime + 10% white tuff waste was determined as 1651.59 kPa. The highest strength after the F-T cycles was obtained from the SLG10 sample containing soil + 6% lime + 10% green tuff waste as 1382.05 kPa. From the statistical analyses determined that there is a significant, positive correlation between HU value and unconfined compressive strength ( $r=0.99$ ,  $p<0.01$ ). As a result of the study, it was determined that waste zeolites decreased swelling pressure, and the one-dimensional swelling percentage of clayey soil increased unconfined compressive strength and durability performances of soil on a limited scale. On the other hand, no swelling behavior was observed in the soils stabilized with lime and lime-waste zeolite mixtures. Mechanical and durability performances of waste zeolite-lime mixtures are more effective than lime-stabilized soils. Strength and durability performances of soils can be estimated accurately considering HU values. In the light of the data obtained from the experimental study, the relationship between unconfined compressive strength and HU values showed that CT is a useful method in the analysis of soil microstructure and nondestructive strength evaluation.

**Keywords** Unconfined compressive strength · CT imaging · Soil stabilization · Freezing–thawing cycles (F-T)

Responsible Editor: Zeynal Abiddin Erguler

✉ Hakan Alper Kamiloğlu  
hkamiloglu@bayburt.edu.tr

Fatih Yılmaz  
fyilmaz@bayburt.edu.tr

Erol Sadoğlu  
esadoglu@ktu.edu.tr

<sup>1</sup> Department of Civil Engineering, Engineering Faculty, Bayburt University, 69010 Bayburt, Turkey

<sup>2</sup> Department of Civil Engineering, Engineering Faculty, Karadeniz Technical University, 61100 Trabzon, Turkey

## Introduction

Freezing–thawing (F-T) and heaving are significant factors causing soil volume change in cold regions. These factors have destructive effects on many engineering applications such as pipelines, highways, embankments, or water conveyance channels (Lu et al., 2019). In cold regions, at least one freezing and thawing cycle occur in a year (Kalkan, 2009; Yarbaşı et al., 2007). The F-T cycles have effects on soil based on physical, chemical, and biological aspects (Liu et al., 2021). The primary reason for the negative effect of

the F-T on the physical and mechanical properties of soil is gradually enlarging void spaces of soil due to frozen moisture in the voids. Besides, the F-T cycles lead to fragmentation of coarse particles and aggregation of fine soil particles (Zhang et al., 2016). In cold regions, engineering behaviors of soil are the most affected parameters by freezing and thawing cycles. There is a wide range of studies examining the effect of F-T on various soil engineering behavior such as density (Konrad, 1989), dynamic properties (Mahya et al., 2021), hydraulic permeability (Viklander, 1998; Yıldız and Soğancı, 2012), stress–strain relation (Eskişar et al., 2015; Lu et al., 2020; Sahlabadi et al. 2021), mechanical properties of soils (Hohmann-Porebska, 2002; Liu et al., 2019; ShahriarKian et al., 2021; Jamshidvand et al. 2021), and dynamic characteristics (Cui et al., 2014; Wang et al., 2015).

Generally, the substantial effects of F-T on soil properties are seen in shallow soil layers due to the low thermal conductivity of the soil. Thus, in most studies, it was recommended to overcome the negative effects of F-T cycles using shallow stabilization methods. Some of the widely used shallow soil stabilization methods based on stabilizers can be categorized as conventional additives (Hotineanu et al., 2015; Saadat and Bayat, 2019; Wu et al., 2020), geofibers and synthetic fluids (Zaimoglu, 2010; Tiwari et al., 2020; Liu et al., 2021), non-conventional chemical additives (Güllü, 2015; Uzer, 2016; Yılmaz and Fidan, 2018; Taş et al. 2018), alkali activated materials (Amulya et al., 2020; Karouzou et al., 2020; Syed et al., 2020), and recycled materials (Aydin et al., 2020; Jafari and Esna-ashari, 2012; Yılmaz et al., 2015).

Zeolite minerals which have a wide range of uses are produced by several countries in the world (Flanagan, 2016). In some studies, it was suggested to use zeolite minerals as a soil stabilization agent (Mola-Abasi and Shooshpasha, 2016; Savas, 2016; Eyo et al., 2020; ShahriarKian et al., 2021; Chenarboni et al., 2021). Bayburt province is one of the places where zeolite-rich tuffs are found in Turkey. The zeolite-rich tuffs are commonly used as restoration or structural materials (Cicerali et al., 2020). Yılmaz et al. (2015) stated that large amounts of waste material are generated during cutting operations, which could be used for soil stabilization.

From the early 1980s, the CT scanning has been used in the civil engineering discipline. As the CT enables to examine 3D structure of soils and is a rapid and non-destructive method, CT scanning to examine soil structure is gradually increasing in geotechnical engineering (Peth et al., 2008; Liu et al., 2021; Xu et al., 2021). CT scanning is used to examine pore morphology (Han et al., 2020), pore size distribution (Akhondzadeh et al., 2020), and micro–macro cracks in soil media (Wang et al., 2020). The pore structure of the soil is a primarily examined factor in geotechnical studies concerning the freezing–thawing effect. Therefore, X-ray and CT scanners are functional to observe and quantify pore

characteristics (Liu et al., 2021). The HU is a dimensionless unit universally used in CT scanning to express CT numbers in a standardized and convenient form. As the HU value is a distinctive parameter in CT scanning, materials can be specified based on the HU values.

Despite chemical and mineralogical structure of the waste zeolites being similar to widely used waste materials in stabilization applications such as fly ash and blast-furnace slug, few study was examined durability performance of the tuffs considering the inner structure. Zeolite-rich tuffs can be mined in various parts of the world, such as Turkey, Greece, Italy, Yemen, Iran, the USA, and Japan (Kitsopoulos et al., 1996; Pham et al., 2019; Rajabi and Ardakani, 2020). The studies showed that there are little differences in oxide components and mineralogical structures between these tuffs (Eyo et al., 2020; ShahriarKian et al., 2021). The effect of these differences on the mechanical and durability performances of the stabilized samples is a gap in the literature. Thus, three different of subtypes of the tuffite formation was taken into account to examine the effect of differences of tuff structure on the stabilization performance. Ultrasonic pulse velocity (UPV) is one of the widely used nondestructive tests methods. However, UPV values are prone to inconsistencies originating from the experimental process. In a wide range of studies about soil stabilization assessments, CT scanning is used to examine pore structure. On the other hand, there are very few studies on assessing the usability of the HU values as a non-destructive strength assessment method. This study aimed to investigate the effect of waste zeolites on swelling pressure, mechanical properties, and durability of stabilized clayey soil subjected to freezing–thawing cycles. Within this scope, SEM, CT scanning, and image processing methods were used to examine the micro and macro effects of the waste zeolites. The specific objectives of this paper were to (1) investigate statistical significance between unconfined compressive test and HU values of stabilized soils and (2) evaluate the effects of freeze–thaw cycles on HU values and unconfined compressive strengths of the samples.

## Material

### Natural soil

Clayey soil was taken at a depth of 2 m from the trial pit excavated at the Demirözü district of Bayburt city (Turkey). Some of the geotechnical properties of the soil are presented in Table 1.

Grain size distribution, compaction parameters, specific gravity, and Atterberg limits of the soil were determined considering ASTM D 422, ASTM D698, ASTM D 854, and ASTM D 4318, respectively. The grain size distribution of

**Table 1** Physical properties of the soil

Property	Values
Liquid limit, (%)	113.60
Plasticity index, (%)	84.90
Optimum water content, (%)	24.2
Maximum dry density (kN/m <sup>3</sup> )	14.50
Classification (USCS)	CH
Classification (AASHTO)	A-7-5
Specific gravity	2.60
Activity	4.71

the natural soil is presented in Fig. 1a. The organic matter content was determined as 5% (ASTM D 2974). It was seen that the soil is suitable for lime stabilization applications based on the organic matter content. X-ray diffraction (XRD) analysis was performed for natural soil using Rigaku/StamartLab X-Ray diffractometer (ASTM D 5381). The estimated mineralogical composition of the soil is shown in Fig. 1b. Based on the estimation, it is seen that the main mineralogical components of the soil are montmorillonite (M), quartz (Q), and calcite (C).

**Lime and waste zeolites**

In the context of this study, natural soil was stabilized with lime and three types of natural tuff mixtures. Commercially available hydrated lime used in the stabilization was obtained from Karsan Lime Company. X-ray fluorescence (XRF) analyses were performed to determine the oxide composition of the lime and waste zeolites considering ASTM D 934. There are three types of tuffs locally known as Bayburt Stone (BS). The zeolite-rich tuffs are commonly used as restoration or structural materials (Cicerali et al., 2020). During the mining and cutting process, a large amount of waste material occurs. As the average rejection rate is over 60%, disposing of the waste material is required to prohibit environmental pollution. Some of the physical properties and chemical components of lime and the tuffs are given in Table 2. The siliceous nature of the tuffs can be seen from the table, and it is also seen that

**Table 2** Oxide composition and physical properties of lime and the tuffs

	Lime	Tuff-1 (GTW)	Tuff-2 (WTW)	Tuff-3 (YTW)
SiO <sub>2</sub> (%)	0.23	68.22	69.96	70.26
Al <sub>2</sub> O <sub>3</sub> (%)	0.11	12.06	12.25	16.91
Fe <sub>2</sub> O <sub>3</sub> (%)	0.40	1.84	0.33	2.97
CaO (%)	65.00	2.17	2.52	0.37
MgO (%)	1.40	1.04	1.20	0.81
Ca(OH) <sub>2</sub> (%)	85.80	-	-	-
SO <sub>3</sub> (%)	-	0.09	0.05	0.05
K <sub>2</sub> O (%)	-	1.54	2.43	3.29
Na <sub>2</sub> O (%)	-	6.08	0.57	0.30
Loss of ignition	-	6.79	10.08	4.25
Physical properties				
> 75 μ (%)	3.8	-	-	-
> 45 μ (%)	-	5.0	7.0	5.0
Specific gravity	2.37	2.30	2.32	2.50
pH	12.4	-	-	-
Blaine (cm <sup>2</sup> /g)	-	6250	7194	7364
Pozzolanic activity	-	10.5	8.8	1.4
Color	White	Green	White	Yellow

SiO<sub>2</sub>, Al<sub>2</sub>O<sub>3</sub>, and Fe<sub>2</sub>O<sub>3</sub> oxides contain more than 80% of the total compound. The tuffs do not contain harmful chemical matters such as nitrate, sulfate, radioactive elements, or heavy metals. Therefore, it can be qualified as a harmless soil stabilization agent.

Color is the most notable distinctive feature of the tuff types. In Table 2, green (GTW), white (WTW), and yellow waste zeolites (YTW) are denoted as Tuff-1, Tuff-2, and Tuff-3, respectively. Within the scope of the study, waste zeolites shown in Fig. 2a were grinded, and the effect of powdered waste zeolites (Fig. 2a) on mechanical and durability properties of stabilized soil was investigated.

**Fig. 1** a Grain size distribution of the natural soil. b X-ray diffraction pattern of the natural soil

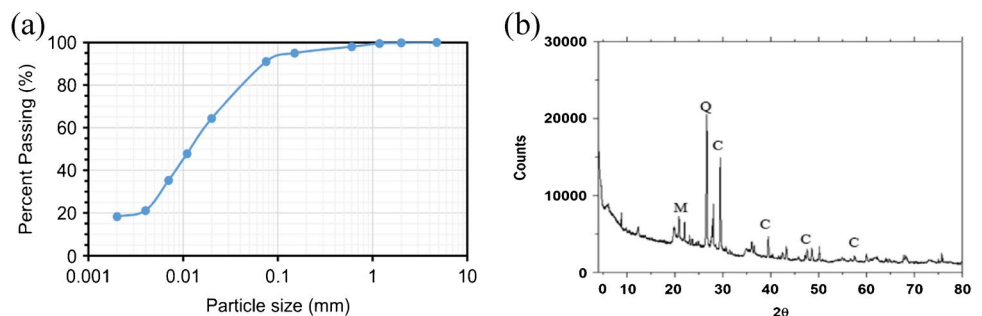
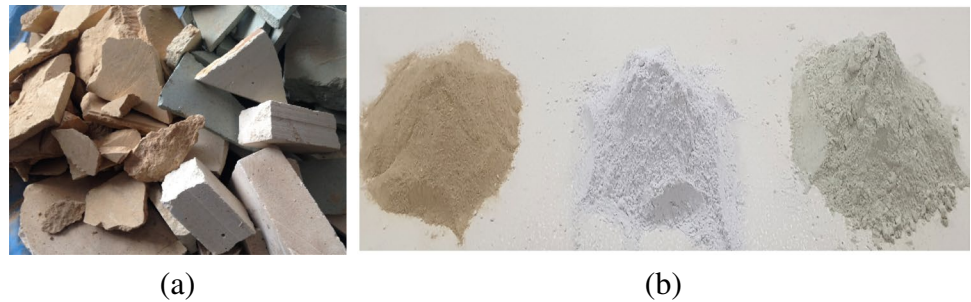


**Fig. 2** Tuff wastes used in the study. **a** Raw tuff wastes. **b** Powdered tuff wastes



As one of the major components is zeolitic materials, the tuffs contain a high silica structure. XRD patterns of the powdered waste zeolites are shown in Fig. 3. The chief mineralogical components of the tuffs are quartz (Q), feldspar (F), and periclase (P) for GWT and WWT (Fig. 3a and b), quartz (Q), and feldspar (F) for YWT (Fig. 3c).

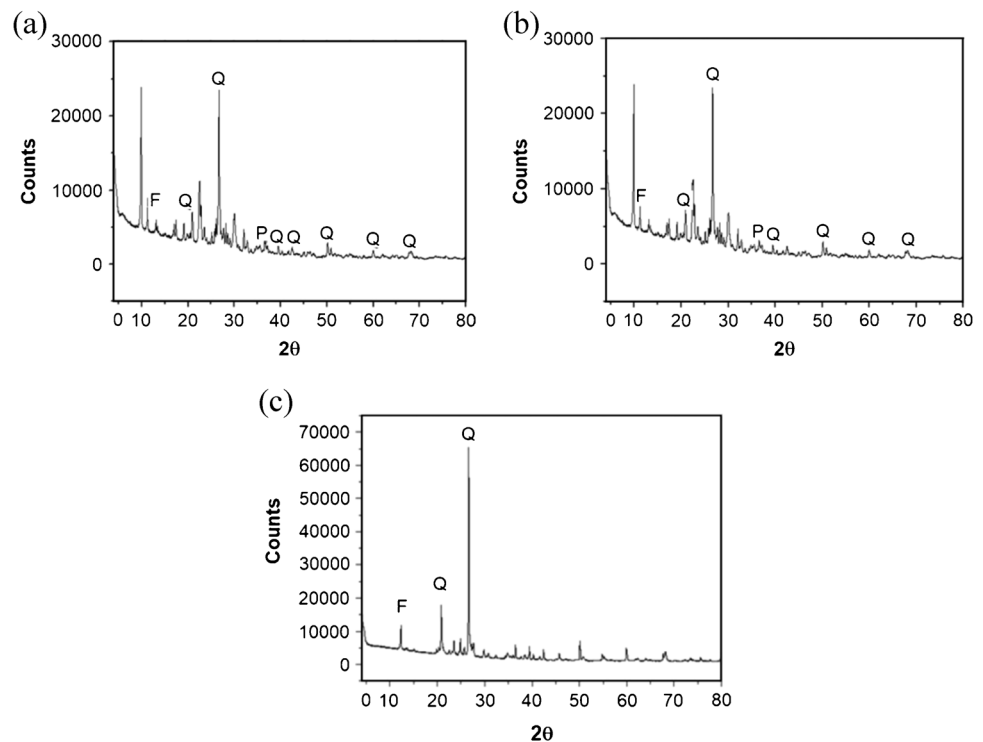
### Sample preparation

Soil-tuff and soil-tuff-lime mixtures were prepared considering optimum water content. Pulverized tuff was used in the stabilization applications. The pulverization of the tuff wastes was done with stone crushing and grinding machines. The grinding process was continued until 90% of the grains were under 100-micron material. Stabilization studies were started after obtaining 90% of the material below 100 microns with the granulometry analysis. The pulverized tuff and optimum amount of lime were mixed in the Hobart

mixer for 5 min. The pH value of the samples was taken into account to determine the optimum amount of lime. Suspensions of the mixtures were prepared by adding lime to the natural soil at an increasing rate of 1% between 0 and 10%, in the test carried out at a pH measurement temperature of 21.7 °C. The optimum lime ratio criterion was taken as 12.4, the pH value of the lime and water solution. The minimum lime ratio value corresponding to this value in natural sample and lime mixture solutions was determined as the optimum lime ratio of the soil (6%). The prepared mixture was mixed with soil for 5 min. The dry matters were mixed with a predetermined amount of water and mixed for 5 min to sustain homogeneity.

The mixtures were compacted into a standard compaction mold with standard compaction energy. Samples used for various tests are taken from the mold using special thin wall samplers. Cylindrical samples of 76 mm length and 38 mm diameter were used for unconfined compressive strength,

**Fig. 3** X-ray diffraction patterns of **a** green waste zeolites (GWS), **b** white waste zeolite (WWT), **c** yellow waste zeolite (YWT)



durability tests, and CT imaging. The 20 mm length and 75 mm diameter specimens were used for swelling pressure and one-dimensional swelling percentage tests. The samples were wrapped with plastic film and cured for 28 days (unconfined compressive strength, durability tests, and CT imaging) or 14 days (swelling pressure and one-dimensional swelling percentage tests) under constant humidity ( $97\% \pm 2\text{ }^\circ\text{C}$ ) and temperature ( $20\text{ }^\circ\text{C} \pm 3\text{ }^\circ\text{C}$ ).

### Method

At the first stage of the study, optimum lime content for stabilizing the soil was determined as 6%, considering ASTM D 6276. The waste zeolites were grinded, and percentages of tuffs by dry weight of soil were determined. In the study, soil and lime were represented with S and L. In the definition of the tuffs, color (G: green, W: white, and Y: yellow) and additive percentage (5%, 10%, 15%, and 20%) were taken into account. Notations used to procure detailed information about the samples are given in Table 3.

### Mechanical properties and durabilities

The optimum moisture content ( $w_{opt}$ ) and maximum dry density ( $\rho_{max}$ ) of the mixtures were determined with standard compaction test (ASTM D 698). Liquid limits ( $w_L$ ), plastic limits ( $w_p$ ), and plasticity index (PI) of the mixture were determined considering ASTM D 4318. Optimum moisture content was considered in [sample preparation](#).

In the context of the study, the effect of waste zeolite amount on unconfined strength and durability parameters was investigated. Within this scope, natural soil, soil-waste zeolite, soil-lime, and soil-lime-waste zeolite mixtures are taken into account. After a 28-day curing period, unconfined compressive strengths of the samples

were determined (ASTM D 2166). The soil samples were subjected to 12 F-T cycles (ASTM D 560) to investigate durability properties of the stabilized soils. Immediately, after F-T cycles, CT imaging was performed and unconfined strengths of samples were determined. Closed system freezing–thawing device was used to subject F-T cycles. The specimens were subjected to freezing at  $-23\text{ }^\circ\text{C}$  for 24 h and then thawing phase  $+21\text{ }^\circ\text{C}$  for 24 h. One F-T cycle comprises freezing and thawing phases.

The effect of waste zeolite on the volumetric change of stabilized soil was investigated with swelling tests. Swelling pressure and free swell index tests were performed on soil (S), soil-waste zeolite (SW, SG, and WY), soil-lime (SL), and soil-lime-waste zeolite (SLW, SLG, and SLY) mixtures considering ASTM D 4546.

### CT and SEM imaging

Besides mechanical properties, CT scanning and SEM imaging were performed to examine the effect of F-T on volume change and pore characteristics of samples. CT scanning was performed with Toshiba Alexion industrial tomograph. Energy levels of 100 kV and 200 mA were applied for scanning. Each sample was divided approximately 152 pieces of slices (0.5 mm slice thickness) with  $512 \times 512$  pixels. The volume and HU value of each sample were determined with 3D Doctor software using image processing technique. Boundary conditions and HU values of the sections were determined as shown in Fig. 4. The HU values of the samples were determined as average HU value of the sections. Characteristic HU value of the 28-day cured samples was determined before and after the F-T cycles.

As enlarging pore size is the primary reason for strength loss originating from F-T cycles, the effect of

**Table 3** Notations used in the experimental study

Combination	Notation	Combination	Notation
Soil	S	Soil, 5%, lime, white zeolite	SLW5
Soil, 5% white zeolite	SW5	Soil, 10%, lime, white zeolite	SLW10
Soil, 10% white zeolite	SW10	Soil, 15%, lime, white zeolite	SLW15
Soil, 15% white zeolite	SW15	Soil, 20%, lime, white zeolite	SLW20
Soil, 20% white zeolite	SW20	Soil, 5%, lime, yellow zeolite	SLY5
Soil, 5% yellow zeolite	SY5	Soil, 10%, lime, yellow zeolite	SLY10
Soil, 10% yellow zeolite	SY10	Soil, 15%, lime, yellow zeolite	SLY15
Soil, 15% yellow zeolite	SY15	Soil, 20%, lime, yellow zeolite	SLY20
Soil, 20% yellow zeolite	SY20	Soil, 5%, lime, green zeolite	SLG5
Soil, 5% green zeolite	SG5	Soil, 10%, lime, green zeolite	SLG10
Soil, 10% green zeolite	SG10	Soil, 15%, lime, green zeolite	SLG15
Soil, 15% green zeolite	SG15	Soil, 20%, lime, green zeolite	SLG20
Soil, 20% green zeolite	SG20		



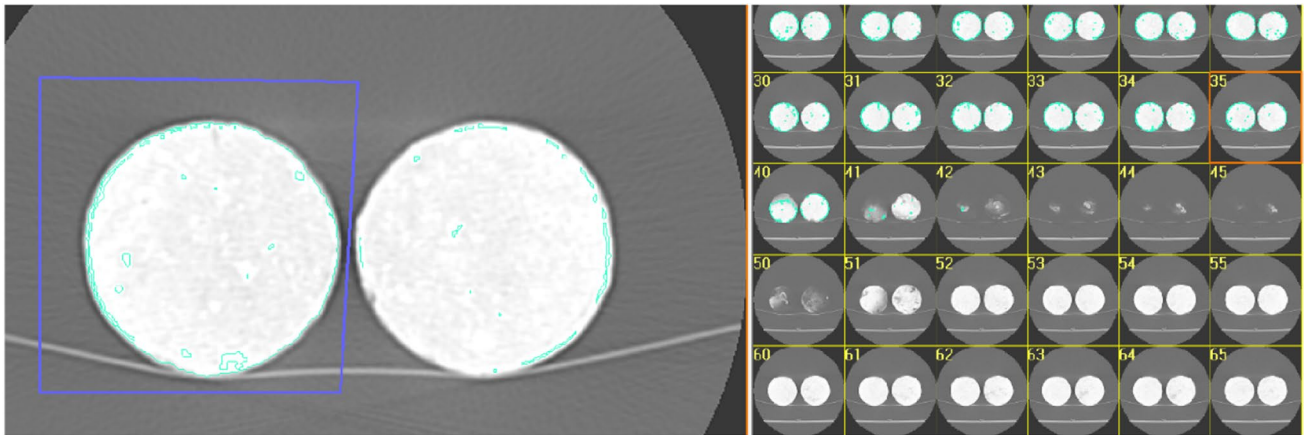


**Fig. 4** Determination of boundary condition of the scanned samples

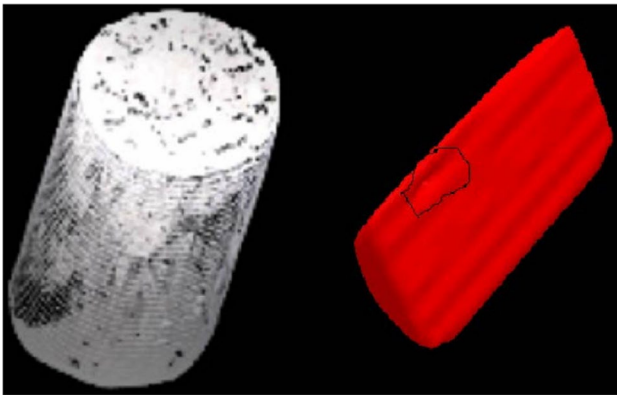


**Fig. 5** Determination of pores of the sample

waste zeolite on the volume change of stabilized soil was investigated. In the context of the study, the volume change of the samples was examined with CT imaging. Volumes of the samples were calculated considering pore volumes with digital image processing software (3D doctor), as it is shown in Fig. 5. The effects of curing time and F-T cycles on volume change of natural soil (S), soil–lime (SL), and soil–lime–waste zeolite (SLW) mixtures were investigated. Volumes of the 1-day cured and 28-day cured samples were determined to examine the effect of curing on volume. The volume of the 28-day cured samples subjected to the F-T cycles was determined to examine the durability performance of the waste zeolites.

Scanning electron microscope (SEM) images of the soil–lime (SL) and soil–lime–waste zeolite (SLW) mixtures

were analyzed to examine the effect of curing (28 days) and F-T cycles on the mechanism of small scale behavior of waste zeolite and lime mixtures in the stabilized soil. The analyses were conducted using Zeiss EQV LS-10 electron microscope.

### Statistical analyses

The HU values (F-Ts) of the stabilized soils were determined from the CT scanning, and statistical significance between HU values and unconfined compressive strength was examined with SPSS 18.0 statistical software. Analysis of variance was performed in the evaluation of the values. Pearson's correlation analysis and Spearman's Rho were performed to measure the strength of association between two variables.

## Results and discussion

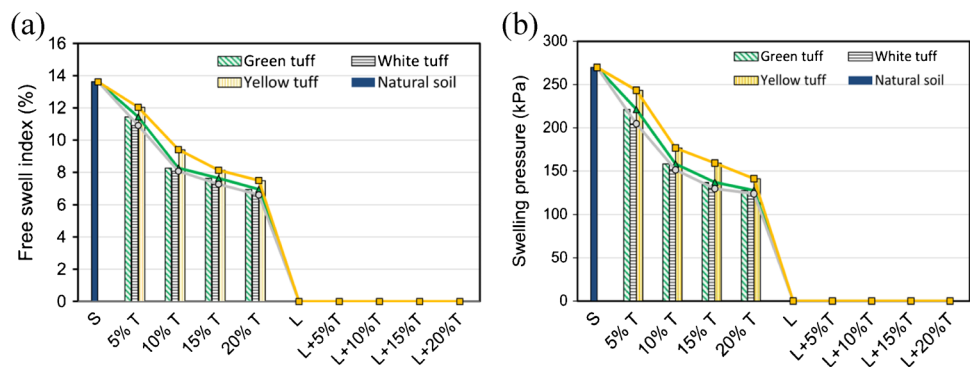
### The effect of waste zeolite and lime on compaction parameters and consistency limits

Compaction parameters and consistency limits of the soil, soil–lime, and soil–lime–waste zeolite mixtures are shown in Table 4. The liquid limit and plasticity index of the soil–waste zeolite mixtures decreased with increasing tuff content. Sharp decrease of liquid limit and plasticity index values were seen in lime-stabilized soil, and lower  $w_L$  and PI values were obtained with soil–lime–waste zeolite mixtures. Waste zeolite waste zeolite–lime mixtures lead to a small amount of decrease in maximum dry unit weight and optimum moisture content of stabilized soils.

**Table 4** Percentage of tuff and lime used in mixture preparation and some physical properties of the mixture

Sample	Tuff (%)	Lime (%)	$\gamma_{max}$ (kN/m <sup>3</sup> )	w <sub>opt</sub> (%)	w <sub>L</sub> (%)	w <sub>p</sub> (%)	PI (%)
S	-	-	15.50	24.20	113.6	28.7	84.90
SG5	5	6	14.72	24.00	112.7	25.3	87.4
SG10	10	6	14.81	23.90	103.9	24.8	79.1
SG20	20	6	15.03	23.50	88.0	23.9	64.1
SW5	5	6	14.69	24.10	108.4	26.9	81.5
SW10	10	6	14.93	23.90	107.5	26.4	81.1
SW15	15	6	15.01	22.40	99.2	26.0	73.2
SW20	20	6	15.26	21.20	96.8	25.6	71.2
SY5	5	6	14.62	23.90	110.4	26.3	84.1
SY10	10	6	14.79	23.70	107.6	25.4	82.2
SY15	15	6	14.83	22.20	104.8	24.8	80.0
SY20	20	6	14.92	21.60	93.3	24.1	69.2
SL	0	6	14.42	27.80	78.6	42.1	36.5
SLG5	5	6	14.44	25.10	77.6	40.7	36.9
SLG10	10	6	14.44	24.90	73.8	38.5	35.3
SLG15	15	6	14.59	24.10	72.4	38.2	34.2
SLG20	20	6	14.67	23.90	70.6	37.5	33.2
SLW5	5	6	14.47	25.60	77.3	40.9	36.4
SLW10	10	6	14.61	24.00	78.1	41.3	36.8
SLW15	15	6	14.79	23.80	76.4	39.6	36.8
SLW20	20	6	15.02	23.10	75.2	39.3	35.9
SYG5	5	6	14.37	24.70	78.4	41.1	36.5
SLY10	10	6	14.49	23.80	76.9	41.0	35.9
SLY15	15	6	14.52	22.00	75.3	40.1	35.2
SLY20	20	6	14.63	21.70	72.9	39.4	33.5

**Fig. 6** The effect of waste zeolite, lime, and waste zeolite-lime mixtures on **a** free swell index of samples and **b** swelling pressure of samples



**The effect of waste zeolite content on swelling characteristics of stabilized soil**

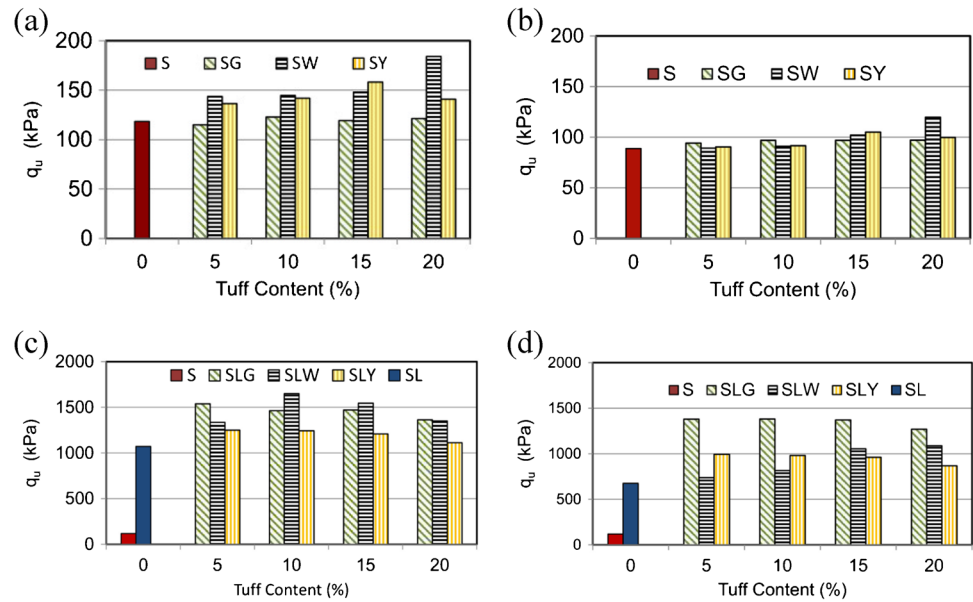
Swelling pressure tests were performed on natural soil (S), soil-waste zeolite mixtures (SW), and soil-lime-waste zeolite mixtures cured for 14 days at 20 °C. Figure 6a and b show the effect of waste zeolite and lime on free swell index and swelling pressure, respectively. From the figures, it was seen that free swell index and swelling pressure decreases with increasing tuff content, and lime plays a decisive role on swelling characteristics.

Lime and lime-waste zeolite mixtures lead to eliminate the volumetric behavior of soil.

**The effect of F-T cycles on unconfined compressive strength**

In this part of the study, the effect of the amount of tuff wastes on unconfined compressive strength was examined. Within this scope, a high plasticity clayey soil was stabilized waste zeolite and lime-waste zeolite mixtures with various tuff contents. Unconfined compressive strengths of

**Fig. 7** Unconfined compressive strength of the samples **a** stabilized with waste zeolite before the F-T cycles, **b** stabilized with waste zeolite after the F-T cycles, **c** stabilized with waste zeolite-lime mixtures before the F-T cycles, and **d** stabilized with waste zeolite-lime mixtures after the F-T cycles



soil (S) and soil-waste zeolite mixture (SG, SW, SY) are presented in Fig. 7a. A slight increase in unconfined compressive strength was observed with increasing waste zeolite amount. A similar trend in USC values was observed in ShahriarKian et al. (2021). In this study, it was intended to stabilize a low plasticity soil with zeolite, cement, and cement-zeolite mixtures. UCS values of the soil-zeolite mixture were higher with respect to the soil. In both of the studies, a slight increase in UCS can be explained by the role of materials. Natural tuff and zeolite acted as filler material.

Besides, durability performances of the waste zeolites were investigated by subjecting the samples to strength tests after F-T cycles. In Fig. 7b, unconfined compressive strengths of the mixtures after subjecting F-T cycles were shown. The strength of the waste zeolite-soil mixture showed better performance than natural soil. However, a notable increment of unconfined strength and durability was not observed.

Unconfined compressive strength of natural soil (S), soil-lime (SL), soil-lime-waste green tuff (SLG), soil-lime-waste white tuff (SLW), and soil-lime-waste yellow tuff (SYG) mixtures are presented in Fig. 7c. From the figure, it was seen that waste zeolite increased the unconfined compressive strength of the samples up to 50%. The reason for the strength increment can be explained by containing a high amount of  $\text{SiO}_2$ ,  $\text{Al}_2\text{O}_3$ , and  $\text{Fe}_2\text{O}_3$  oxides of waste zeolites. The strength increased with increasing tuff content up to a constant rate; beyond this rate, strength of the samples decreased with increased tuff content. Optimum contents of the SLG, SLW, and SLY are 5%, 10%, and 5% respectively. The effect of zeolite-rich material on the UCS value of the samples becomes more explicit when they are mixed with

CaO supply such as cement or lime. Figure 7c is compatible with the findings of ShahriarKian et al. (2021) and Chenarbonei et al., (2021). These studies show that the cement-zeolite mixture increases the UCS values, and zeolite has positive effects on the UCS values of the stabilized samples.

It can be seen from Fig. 7d that tuff wastes reduce the negative effects of F-T cycles on strength. This finding is compatible with ShahriarKian et al. (2021) and Jamshidvand et al. (2021). These studies show that zeolite or zeolite-rich tuff alleviates the negative effects of F-T cycles on strength. It is apparent from this figure that the strength reduction of lime and SLW mixture is the lowest. Because yellow waste zeolite contains much more  $\text{Na}_2\text{O}$  than other types of tuffs, NaOH is formed as a result of the reaction of  $\text{Na}_2\text{O}$  with water. The NaOH leads to an increase pH value of the soil media and increases the stability of CSH products.

### Macro-microstructure of the samples

This part of the study was intended to investigate the relation between the microstructure of the soil samples and unconfined compressive strengths. The HU value was considered in the evaluation of the macrostructure of the samples. The HU values of the 28-day cured samples before and after the F-T cycles were determined. The determined HU values of soil (S), soil-lime (SL), soil-lime-waste green tuff (SLG), soil-lime-waste white tuff (SLW), and soil-lime-waste yellow tuff (SYG) mixtures are presented in Fig. 7a. After subjecting F-T cycles, the HU values of the 28-day cured samples were determined, as it is shown in Fig. 7b. From Figs. 6 and 7, it was seen that tendency of the HU value and unconfined compressive strengths was similar.



**Fig. 8** HU values of samples **a** stabilized with waste zeolite before the F-T cycles, **b** stabilized with waste zeolite after the F-T cycles, **c** stabilized with waste zeolite-lime mixtures before the F-T cycles, and **d** stabilized with waste zeolite-lime mixtures after the F-T cycles

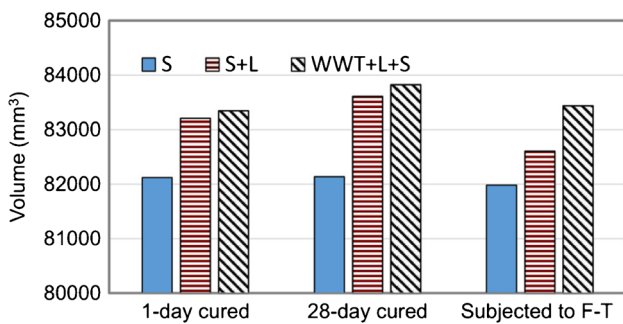
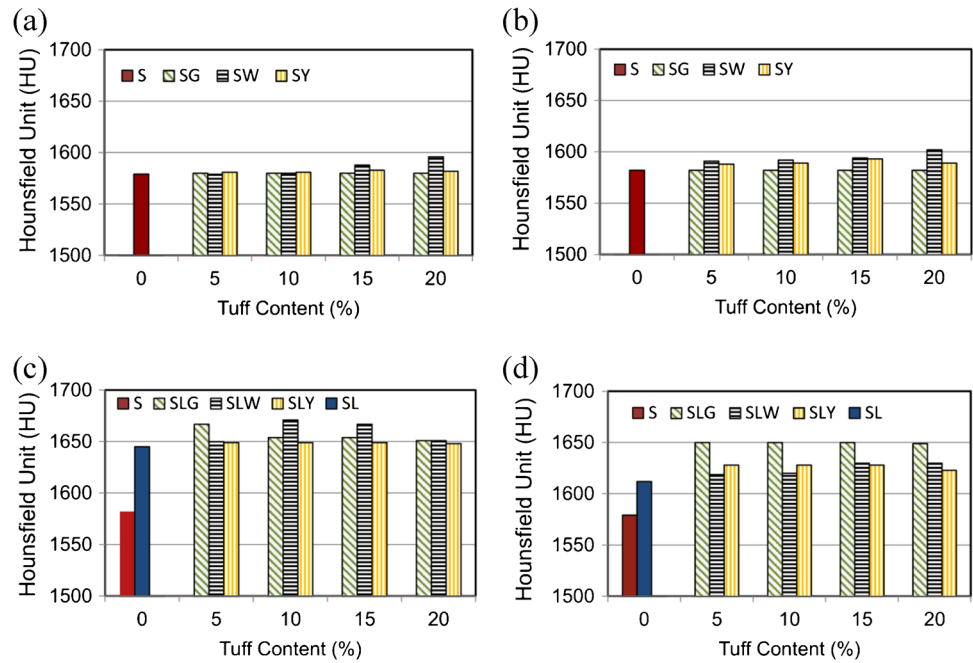


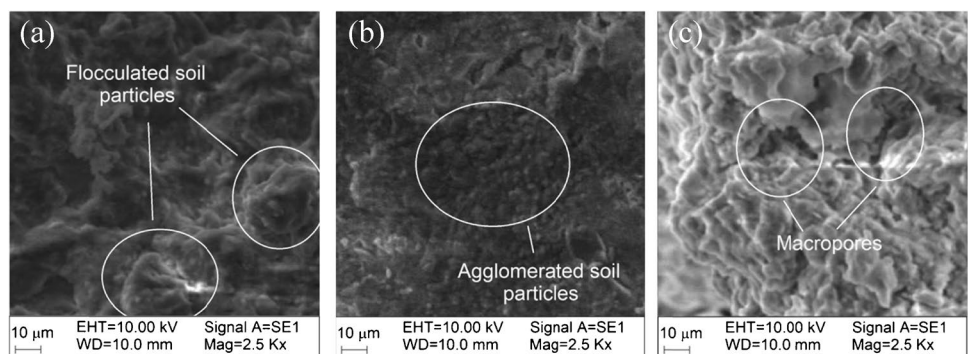
**Fig. 9** The effect of curing time and C-T cycles on volume change of the samples

Simple correlation analyses were performed to examine statistical significance between unconfined compressive strength and HU values before and after the F-T cycles. As a result of the Spearman’s rho test, it was determined that there is a significant, positive correlation between

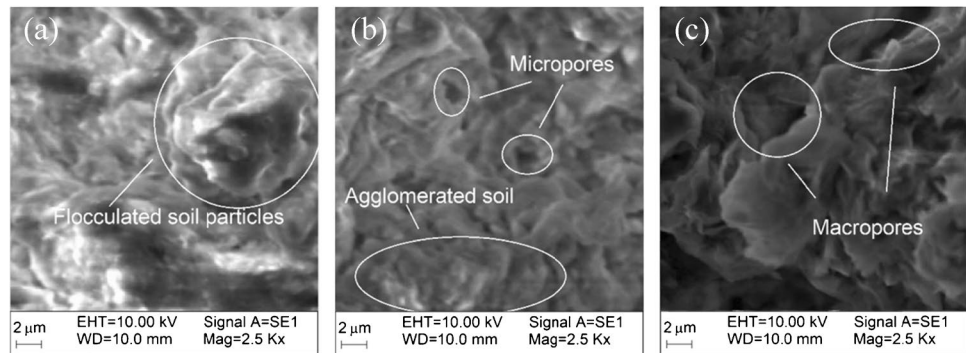
HU value and unconfined compressive strength ( $r=0.99$ ,  $p < 0.01$ ). Regression analyses were performed to examine the statistical predictability of unconfined compressive strength using HU values. As a result of ANOVA, it was determined that unconfined compressive strength could be estimated using HU values ( $r = 0.96$ ,  $r^2 = 0.93$ ,  $p < 0.01$ ).

Figure 9 shows the effect of curing time and amount of waste zeolite on the volume change of stabilized soils. From the figure, it was seen that volumes of the SK and SLW samples increased with curing time. Volumetric increment of the solid phase of the samples can be explained with synthesized high strength materials as a result of pozzolanic reactions by considering the increase of strength and HU value shown in Figs. 7 and 8, respectively. F-T cycles decreased the volume of all samples. By considering HU loss in Fig. 7b, the volumetric reduction can be explained with an increment of pore size. From Fig. 9, it was seen that waste zeolites are effective on volumetric stability of soils.

**Fig. 10** SEM images of SL samples **a** 1-day cured samples, **b** 28-day cured samples before F-T cycles, and **c** 28-day cured samples after F-T cycles ( $\times 2500$ )



**Fig. 11** SEM images of SLW samples **a** 1-day cured samples, **b** 28-day cured samples before F-T cycles, and **c** 28-day cured samples after F-T cycles ( $\times 5000$ )



In this part of the study, the effects of the curing period and F-T cycles on the microstructure of the samples were investigated. Within this scope, the microstructures of the SL and SLW samples were considered. SEM images of the 1-day cured samples and 28-day cured samples (before and after C-T cycles) were examined. Figures 10 and 11 show SEM images of the lime-treated soil. From Figs. 10a and b and 11a and b, flocculation and agglomeration phases of stabilized soil are seen. As seen from Fig. 10b, flocculated and agglomerated particles lead to an increase in the volume of the solid structure. Thus HU value and unconfined strength of the samples increased. From Figs. 10c and 11c, it is seen that F-T cycles caused an increase of pore dimensions. Thus, HU values and the strength of the samples subjected to F-T cycles decreased (Figs. 7 and 8).

## Conclusions

This paper investigated the durability performances of stabilized high plasticity clayey soil with lime and waste zeolites additives. The contribution of additives was examined in macro and micro aspects. In this context, unconfined compressive strength, CT, and SEM images were taken into account. The following conclusions can be drawn from the results of the test:

- HU values and unconfined compressive strength of the lime-stabilized samples increased remarkably with the curing period. Waste zeolite-lime mixtures showed better performance than lime-stabilized soils based on unconfined compressive performance. From the XRF, XRD, CT imaging, and unconfined compressive strength results, it was seen that waste zeolite contributed to pozzolanic reactions that occurred in the lime-stabilized samples due to comprising a high amount of active pozzolanic oxide components. CSH gels formed in the pores of the soil particles due to pozzolanic reactions between lime and waste zeolites. Volumetric increment of the samples can be explained with a new material synthe-

sized between the soil particles. HU values increased depending on synthesized solid material, and increased UCS value confirmed that high strength material formed as a result of pozzolanic reactions.

- Waste zeolite and lime mixture increased the UCS values up to 53% in comparison to lime-stabilized samples. Little differences in oxide composition of waste zeolites may affect mechanical, and durability performances of samples stabilized with lime and waste zeolites. Lime and white waste zeolite mixture showed a remarkable improvement in the UCS value. A similar trend was observed between the UCS and HU values.
- The SEM analyses determined that the inner structure of the soils stabilized lime and waste zeolite mixture were denser than lime-stabilized soils. F-T cycles led to enlarge pore size. Adding waste zeolites led to increasing durability performance of soils stabilized with lime. Lime-green waste zeolite mixtures showed the best performance against freezing–thawing cycles. Although the UCS value of the lime-stabilized soil decreased 35% due to F-T cycles, the strength loss of the stabilized soils with lime and green waste zeolite mixture was 12.5%. Additionally, the UCS value of the samples subjected to F-T cycles was 33% higher than lime-stabilized soils did not subject to F-T cycles.
- The strength of soils can be evaluated accurately considering HU values. As a result of the Spearman's rho test, it was determined that there is a significant, positive correlation between HU value and unconfined compressive strength ( $r=0.99$ ,  $p < 0.01$ ). Considering the ANOVA results, it was determined that unconfined compressive strength can be estimated using HU values ( $r=0.96$ ,  $r^2=0.93$ ,  $p < 0.01$ ).
- CT imaging has a considerable advantage in geotechnical applications due to giving an opportunity to examine 3D structures and evaluate the strength performances of soils without any disturbance.

The stabilizing behavior of tuff wastes with and without lime in various types of natural materials can be

researched in future studies. Instead of lime, another major binder can be utilized. Experiments carried out in the laboratory can be backed up by field tests.

**Acknowledgements** This research has been supported by Bayburt University Scientific Research Project Coordination Department. (Project No: 2018/01-69001-29 and 2014/01-04).

**Data availability** Some or all data, models, or code that support the findings of this study are available from the corresponding author upon reasonable request.

## Declarations

**Conflict of interest** The author declares no competing interests.

## References

- Akhondzadeh H, Keshavarz A, Al-Yaseri AZ, Ali M, Awan FUR, Wang X, Yang Y, Iglauer S, Lebedev M (2020) Pore-scale analysis of coal cleat network evolution through liquid nitrogen treatment: a micro-computed tomography investigation. *Int J Coal Geol* 219:103370. <https://doi.org/10.1016/j.coal.2019.103370>
- Amulya S, Ravi Shankar AU, Praveen M (2020) Stabilisation of lithomargic clay using alkali activated fly ash and ground granulated blast furnace slag. *Int J Pavement Eng* 21:1114–1121. <https://doi.org/10.1080/10298436.2018.1521520>
- Aydin K, Sivrikaya O, Uysal F (2020) Effects of curing time and freeze–thaw cycle on strength of soils with high plasticity stabilized by waste marble powder. *J Mater Cycles Waste Manag* 22:1459–1474. <https://doi.org/10.1007/s10163-020-01035-0>
- Chenarboni HA, Lajevardi SH, MolaAbasi H, Zeighami E (2021) The effect of zeolite and cement stabilization on the mechanical behavior of expansive soils. *Constr Build Mater* 272:121630. <https://doi.org/10.1016/j.conbuildmat.2020.121630>
- Ciceralli D, Arslan M, Abdioğlu Yazar E, Yücel C, Temizel İ, Park S, Schroeder PA (2020) Mineralogy, chemistry, and genesis of zeolitization in Eocene tuffs from the Bayburt area (NE Turkey): constraints on alteration processes of acidic pyroclastic deposits. *J African Earth Sci* 162:103690. <https://doi.org/10.1016/j.jafrearsci.2019.103690>
- Cui Z-D, He P-P, Yang W-H (2014) Mechanical properties of a silty clay subjected to freezing–thawing. *Cold Reg Sci Technol* 98:26–34. <https://doi.org/10.1016/j.coldregions.2013.10.009>
- Eskişar T, Altun S, Kalıpcılar İ (2015) Assessment of strength development and freeze–thaw performance of cement treated clays at different water contents. *Cold Reg Sci Technol* 111:50–59. <https://doi.org/10.1016/j.coldregions.2014.12.008>
- EU EyoNg'ambi, S., Abbey, S.J., 2020 Performance of clay stabilized by cementitious materials and inclusion of zeolite/alkaline metals-based additive *Transp Geotech* 23 <https://doi.org/10.1016/j.tgeo.2020.100330>
- Flanagan, D.M., 2019. Mineral commodity summaries. Virginia.
- Güllü H (2015) Unconfined compressive strength and freeze–thaw resistance of fine-grained soil stabilised with bottom ash, lime and superplasticiser. *Road Mater Pavement Des* 16:608–634. <https://doi.org/10.1080/14680629.2015.1021369>
- Q Han H Bai L Liu Y Zhao Y Zhao 2020 Model representation and quantitative analysis of pore three-dimensional morphological structure based on soil computed tomography images *Eur J Soil Sci*<https://doi.org/10.1111/ejss.13072>
- Hohmann-Porebska M (2002) Microfabric effects in frozen clays in relation to geotechnical parameters. *Appl Clay Sci* 21:77–87. [https://doi.org/10.1016/S0169-1317\(01\)00094-1](https://doi.org/10.1016/S0169-1317(01)00094-1)
- Hotineanu A, Bouasker M, Aldaood A, Al-Mukhtar M (2015) Effect of freeze–thaw cycling on the mechanical properties of lime-stabilized expansive clays. *Cold Reg Sci Technol* 119:151–157. <https://doi.org/10.1016/j.coldregions.2015.08.008>
- Jafari M, Esna-ashari M (2012) Effect of waste tire cord reinforcement on unconfined compressive strength of lime stabilized clayey soil under freeze–thaw condition. *Cold Reg Sci Technol* 82:21–29. <https://doi.org/10.1016/j.coldregions.2012.05.012>
- S JamshidvandA Ardakani A Kordnaej 2021 Effect of cement and zeolite on silty sand samples under freeze–thaw cycles *Road Mater Pavement Des* 1–24 <https://doi.org/10.1080/14680629.2021.1924238>
- Kalkan E (2009) Effects of silica fume on the geotechnical properties of fine-grained soils exposed to freeze and thaw. *Cold Reg Sci Technol* 58:130–135. <https://doi.org/10.1016/j.coldregions.2009.03.011>
- Karozou A, Konopisi S, Pavlidou E, Stefanidou M (2020) Long-term behavior and durability of alkali-activated clay mortars. *Materials (basel)* 13:3790. <https://doi.org/10.3390/ma13173790>
- Kitsopoulos KP, Dunham AC (1996) Heulandite and mordenite-rich tuffs from Greece: a potential source for pozzolanic materials. *Miner Depos* 31:576–583. <https://doi.org/10.1007/BF00196138>
- Konrad J-M (1989) Physical processes during freeze–thaw cycles in clayey silts. *Cold Reg Sci Technol* 16:291–303. [https://doi.org/10.1016/0165-232X\(89\)90029-3](https://doi.org/10.1016/0165-232X(89)90029-3)
- Liu B, Ma R, Fan H (2021) Evaluation of the impact of freeze–thaw cycles on pore structure characteristics of black soil using X-ray computed tomography. *Soil Tillage Res* 206:104810. <https://doi.org/10.1016/j.still.2020.104810>
- Liu Y, Wang Q, Liu S, ShangGuan Y, Fu H, Ma B, Chen H, Yuan X (2019) Experimental investigation of the geotechnical properties and microstructure of lime-stabilized saline soils under freeze–thaw cycling. *Cold Reg Sci Technol* 161:32–42. <https://doi.org/10.1016/j.coldregions.2019.03.003>
- Lu Y, Liu S, Alonso E, Wang L, Xu L, Li Z (2019) Volume changes and mechanical degradation of a compacted expansive soil under freeze–thaw cycles. *Cold Reg Sci Technol* 157:206–214. <https://doi.org/10.1016/j.coldregions.2018.10.008>
- Lu Y, Liu S, Zhang Y, Li Z, Xu L (2020) Freeze–thaw performance of a cement-treated expansive soil. *Cold Reg Sci Technol* 170:102926. <https://doi.org/10.1016/j.coldregions.2019.102926>
- Mola-Abasi H, Shooshpasha I (2016) Influence of zeolite and cement additions on mechanical behavior of sandy soil. *J Rock Mech Geotech Eng* 8:746–752. <https://doi.org/10.1016/j.jrmge.2016.01.008>
- Peth S, Horn R, Beckmann F, Donath T, Fischer J, Smucker AJM (2008) Three-dimensional quantification of intra-aggregate pore-space features using synchrotron-radiation-based microtomography. *Soil Sci Soc Am J* 72:897–907. <https://doi.org/10.2136/sssaj2007.0130>
- Pham VT, Meng P, Bui PT, Ogawa Y, Kawai K (2020) Effects of Shirasu natural pozzolan and limestone powder on the strength and aggressive chemical resistance of concrete. *Constr Build Mater* 239:117679. <https://doi.org/10.1016/j.conbuildmat.2019.117679>
- Qi J, Vermeer PA, Cheng G (2006) A review of the influence of freeze–thaw cycles on soil geotechnical properties. *Permafrost Periglacial Process* 17:245–252. <https://doi.org/10.1002/ppp.559>
- Rajabi AM, Ardakani SB (2020) Effects of natural-zeolite additive on mechanical and physicochemical properties of clayey soils. *J Mater Civ Eng* 32:04020306. [https://doi.org/10.1061/\(ASCE\)MT.1943-5533.0003336](https://doi.org/10.1061/(ASCE)MT.1943-5533.0003336)
- Roustaei, M., Hendry, M., Aghaei, E.A., Bayat, M. (2021). Shear modulus and damping ratio of clay soil under repeated freeze–thaw

- cycles. *Acta Geodyn Geomater*, 18, 71–81. <https://doi.org/10.13168/AGG.2021.0005>
- Saadat M, Bayat M (2019) Prediction of the unconfined compressive strength of stabilised soil by adaptive neuro fuzzy inference system (ANFIS) and non-linear regression (NLR). *Geomech Geoeng* 17(1):80–91. <https://doi.org/10.1080/17486025.2019.1699668>
- ShahriarKian, M., Kabiri, S., Bayat, M., 2021. Utilization of zeolite to improve the behavior of cement-stabilized soil. *Int J Geosynth Ground Eng* 7(2). <https://doi.org/10.1007/s40891-021-00284-9>
- Sahlabadi SH, Bayat M, Mousivand M, Saadat M (2021) Freeze–thaw durability of cement-stabilized soil reinforced with polypropylene/basalt fibers. *J Mater Civ Eng* 33(9):04021232. [https://doi.org/10.1061/\(ASCE\)MT.1943-5533.0003905](https://doi.org/10.1061/(ASCE)MT.1943-5533.0003905)
- Savas H (2016) Consolidation and swell characteristics of dispersive soils stabilized with lime and natural zeolite. *Sci Eng Compos Mater* 26:589–598. <https://doi.org/10.1515/secm-2014-0202>
- Syed M, GuhaRay A, Goel D, Asati K, Peng L (2020) Effect of freeze–thaw cycles on black cotton soil reinforced with coir and hemp fibres in alkali-activated binder. *Int J Geosynth Gr Eng* 6:19. <https://doi.org/10.1007/s40891-020-00200-7>
- Taş M, Fidan D, Yılmaz F (2018) Soil stabilization with fly ash and Bayburt stone. *Bayburt Üniversitesi Fen Bilimleri Dergisi* 1(1):8–14 (in Turkish)
- Tiwari N, Satyam N, Singh K (2020) Effect of curing on micro-physical performance of polypropylene fiber reinforced and silica fume stabilized expansive soil under freezing thawing cycles. *Sci Rep* 10:7624. <https://doi.org/10.1038/s41598-020-64658-1>
- Uzer AU (2016) Evaluation of freezing–thawing cycles for foundation soil stabilization. *Soil Mech Found Eng* 53:202–209. <https://doi.org/10.1007/s11204-016-9386-4>
- Viklander P (1998) Permeability and volume changes in till due to cyclic freeze/thaw. *Can Geotech J* 35:471–477. <https://doi.org/10.1139/t98-015>
- Wang P, Qiao H, Zhang Y, Li Y, Chen K, Feng Q (2020) Three-dimensional characteristics of steel corrosion and corrosion-induced cracks in magnesium oxychloride cement concrete monitored by X-ray computed tomography. *Constr Build Mater* 246:118504. <https://doi.org/10.1016/j.conbuildmat.2020.118504>
- Wang T, Liu Y, Yan H, Xu L (2015) An experimental study on the mechanical properties of silty soils under repeated freeze–thaw cycles. *Cold Reg Sci Technol* 112:51–65. <https://doi.org/10.1016/j.coldregions.2015.01.004>
- Y Wu X Qiao X Yu J Yu Y Deng 2020 Study on properties of expansive soil improved by steel slag powder and cement under freeze–thaw cycles *KSCE J CivEng* <https://doi.org/10.1007/s12205-020-0341-6>
- Xu J, Li Y, Ren C, Wang S, Vanapalli SK, Chen G (2021) Influence of freeze–thaw cycles on microstructure and hydraulic conductivity of saline intact loess. *Cold Reg Sci Technol* 181:103183. <https://doi.org/10.1016/j.coldregions.2020.103183>
- Yarbaşı N, Kalkan E, Akbulut S (2007) Modification of the geotechnical properties, as influenced by freeze–thaw, of granular soils with waste additives. *Cold Reg Sci Technol* 48:44–54. <https://doi.org/10.1016/j.coldregions.2006.09.009>
- Yılmaz, F., Kamiloğlu, H.A., Şadoğlu, E., 2015. Soil stabilization with using waste materials against freezing thawing effect. *Acta Phys. Pol. A* 128, B-392–B-395. <https://doi.org/10.12693/APhysPolA.128.B-392>
- Yıldız M, Soğancı AS (2012) Effect of freezing and thawing on strength and permeability of lime-stabilized clays. *Sci Iran* 19:1013–1017. <https://doi.org/10.1016/j.scient.2012.06.003>
- Yılmaz, F., Fidan, D., 2018. Influence of freeze–thaw on strength of clayey soil stabilized with lime and perlite. *Geomech. Eng.* 14. <http://dx.doi.org/10.12989/gae.2018.14.3.301>
- Zaimoglu AS (2010) Freezing–thawing behavior of fine-grained soils reinforced with polypropylene fibers. *Cold Reg Sci Technol* 60:63–65. <https://doi.org/10.1016/j.coldregions.2009.07.001>
- Zhang Z, Wei MA, Feng W, Xiao D, Hou X (2016) Reconstruction of soil particle composition during freeze–thaw cycling: a review. *Pedosphere* 26:167–179. [https://doi.org/10.1016/S1002-0160\(15\)60033-9](https://doi.org/10.1016/S1002-0160(15)60033-9)